JETIR.ORG ISSN: 2349-5162 | ESTD Year : 2014 | Monthly Issue
JOURNAL OF EMERGING TECHNOLOGIES AND INNOVATIVE RESEARCH (JETIR)
An International Scholarly Open Access, Peer-reviewed, Refereed Journal

Theoretical and Experimental Investigation of Gamma-Ray Shielding Characteristics of Biopolymeric Materials.

Kanchan R. Niras[a*], Kalidas B. Gaikwad[ab], Pravina P. Pawar [a.]

[a*] Department of Physics, Dr. Babasaheb Ambedkar Marathwada University, Chhatrapati Sambhajinagar (MS), 431004, India.

[b]Department of Physics, Deogiri College, Chhatrapati Sambhajinagar (MS), 431005, India.

[a*]Corresponding Author: E-mail: kanchanshete16@gmail.com

Abstract

The growing demand for environmentally friendly and lightweight radiation shielding materials has sparked substantial research into biopolymer-based composites for gamma-ray protection. The Phy-X/PSD software database was used to theoretically explore the gamma-ray shielding effectiveness of four biopolymeric materials, namely chitosan (S1), cellulose (S2), starch (S3), and cisplatin (S4). The shielding characteristics were tested over a photon energy range of 122-1330 keV, which corresponds to routinely used gamma-ray sources. The shielding parameters studied were the mass attenuation coefficient (MAC), linear attenuation coefficient (LAC), half-value layer (HVL), tenth-value layer (TVL), and mean free path. The results showed that as photon energy increased, the MAC and LAC values fell, but the HVL, TVL, and MFP values increased due to a fall in photon interaction probability at higher energies. Among the tested substances, S4 consistently had the highest attenuation coefficients and the lowest HVL, TVL, and MFP values over the energy range evaluated, indicating greater gamma-ray shielding. S4's improved shielding efficiency is due to the inclusion of platinum (Pt), a high atomic number element that considerably boosts photon attenuation. In contrast, the biopolymer samples (S1-S3) had lesser shielding effectiveness, with cellulose (S2) performing marginally better than chitosan (S1) and starch (S3). The findings show that platinum-containing biopolymer composites have outstanding radiation attenuation properties and are interesting options for lightweight, environmentally friendly gamma-ray shielding applications in medicine, industry, and nuclear energy. The current theoretical analysis also serves as a solid foundation for the future design and experimental development of enhanced biopolymer-based radiation shielding materials.

Keywords: Biopolymers; Gamma-ray shielding; Phy-X/PSD; Mass attenuation coefficient; Cisplatin; Radiation protection.

1. Introduction

The widespread use of ionising radiation in medical diagnosis, radiotherapy, nuclear power plants, industrial radiography, agriculture, and scientific research has raised the demand for effective radiation shielding materials. Gamma rays and X-rays have a great penetrating capacity and can cause significant biological harm if exposed to levels that exceed permitted limits. As a result, developing efficient shielding materials has become a critical field of research for ensuring radiation safety for workers, patients, and the environment. Traditional shielding materials, such as lead, tungsten, and concrete, have long been used due to their strong radiation attenuation qualities. However, these materials have significant disadvantages, including high density, brittleness, toxicity, low flexibility, and environmental issues about their manufacture and disposal. These

constraints have prompted researchers to investigate lightweight, environmentally benign, and long-lasting radiation shielding solutions [1-4].

Biopolymers have emerged as attractive options for next-generation radiation shielding materials because they are renewable, biodegradable, biocompatible, non-toxic, and simple to manufacture into films, sheets, and composites. Among the various naturally occurring biopolymers, chitosan ($C_{56}H_{103}N_9O_{39}$), cellulose ($(C_6H_{10}O_5)_n$), and starch ($(C_6H_{10}O_5)_n$) have attracted considerable attention due to their abundant availability, excellent mechanical properties, chemical stability, and the presence of hydroxyl and amino functional groups that facilitate interaction with inorganic fillers. These functional groups allow for strong interfacial bonding with high-atomic-number (high-Z) materials, increasing the structural integrity and radiation attenuation performance of the resultant composites. Furthermore, their cheap cost, environmental sustainability, and ease of production make them appealing polymer matrices for advanced shielding applications in the medical, industrial, and nuclear industries [5-8].

The use of compounds containing heavy metals with large atomic numbers can greatly improve the shielding efficiency of biopolymer-based composites. Cisplatin ($C_{12}H_6N_2Pt$), a platinum-based coordination molecule extensively employed as an anticancer medication, has recently received attention due to platinum's (Z=78) high probability of photon interaction by photoelectric absorption and Compton scattering. The introduction of platinum-containing compounds into biodegradable polymer matrices is projected to improve gamma-ray attenuation, especially in the low- and intermediate-energy areas, while also providing multifunctional properties suited for biological applications. These hybrid biopolymer composites combine the mechanical flexibility and environmental compatibility of natural polymers with the improved radiation attenuation capabilities of high-Z elements, making them a possible alternative to traditional hazardous shielding materials [9-11].

Recent advances in materials science and nanotechnology have hastened the creation of multifunctional biopolymer composites by adding metal oxides, ferrites, rare-earth compounds, and platinum-based materials into natural polymer matrices. These composite materials have higher density, mechanical strength, thermal stability, and radiation shielding efficiency while remaining biodegradable and flexible. Photon interactions with these materials are governed by fundamental mechanisms such as the photoelectric effect, Compton scattering, and pair creation, the contributions of which vary with photon energy and elemental composition. To assess the shielding performance of these biopolymer composites over a wide energy range, radiation interaction parameters such as the mass attenuation coefficient (MAC), linear attenuation coefficient (LAC), half-value layer (HVL), tenth-value layer (TVL), mean free path (MFP), effective atomic number (Z_{eff}), effective electron density (N_{eff}), exposure buildup factor (EBF), and energy absorption buildup factor (EABF) must be evaluated [12-15].

Modern computational tools, including as the NIST XCOM database, Phy-X/PSD software, and Monte Carlo simulation approaches, have become important for properly predicting photon interaction parameters and improving novel shielding material composition prior to experimental confirmation. These methodologies allow for a systematic study of the impacts of chemical composition, density, and photon energy on radiation attenuation behavior, making it easier to design lightweight, flexible, and environmentally sustainable shielding materials with enhanced performance [16,17].

As a result, biopolymer-based composites incorporating chitosan, cellulose, starch, and platinum-containing chemicals such as cisplatin offer a promising class of improved radiation shielding materials. Their biodegradability, mechanical flexibility, chemical stability, environmental friendliness, and improved photon attenuation capability make them promising candidates for diagnostic radiology, radiotherapy, nuclear medicine, radioactive waste management, and personal radiation protection. Continued research into these materials is projected to make a substantial contribution to the development of long-lasting, non-toxic, high-performance shielding systems for future radiation protection technologies.

2. Materials and Method

The current study examines the gamma-ray shielding properties of selected biopolymeric materials, including chitosan ($C_{56}H_{103}N_9O_{39}$), cellulose ($(C_6H_{10}O_5)_n$), starch ($(C_6H_{10}O_5)_n$), and cisplatin ($C_{12}H_6N_2Pt$). The elemental compositions of these materials were determined using their respective molecular formulae, and the corresponding densities were derived from available literature. These data used as input parameters for a theoretical study of radiation shielding properties [18].

The Phy-X/PSD program [19] was used to make theoretical estimates of gamma-ray shielding characteristics. Phy-X/PSD is based on the NIST XCOM photon interaction database and allows for precise measurement of photon interaction parameters for elements, compounds, mixtures, and composite materials over a wide photon energy range. The calculations were performed in the photon energy range of 122-1330 keV, which corresponds to the primary gamma-ray energies released by ^{57}Co (122 keV), ^{133}Ba (356 keV), ^{137}Cs (662 keV), ^{54}Mn (835 keV), ^{22}Na (1275 keV), and ^{60}Co (1173 and 1330 keV).

The fundamental shielding parameters, including the mass attenuation coefficient (MAC), linear attenuation coefficient (LAC), half-value layer (HVL), tenth-value layer (TVL), mean free path (MFP) were calculated using the elemental composition and density of each material in the Phy-X/PSD software [20-22].

The linear attenuation coefficient (μ) was calculated from the mass attenuation coefficient (μ/ρ) using:

$$\mu = \left(\frac{\mu}{\rho}\right)\rho \quad \text{----------(1)}$$

where ρ is the density of the investigated material.

The half-value layer (HVL), tenth-value layer (TVL), and mean free path (MFP) were determined using the following equations [3]:

$$\text{HVL} = \frac{\ln 2}{\mu} = \frac{0.693}{\mu} \quad \text{----------(2)}$$

$$\text{TVL} = \frac{\ln 10}{\mu} = \frac{2.303}{\mu} \quad \text{----------(3)}$$

$$\text{MFP} = \frac{1}{\mu} \quad \text{----------(4)}$$

The calculated shielding parameters were compared as a function of photon energy to evaluate the influence of chemical composition on gamma-ray attenuation and to identify the most suitable biopolymeric material for radiation shielding applications.

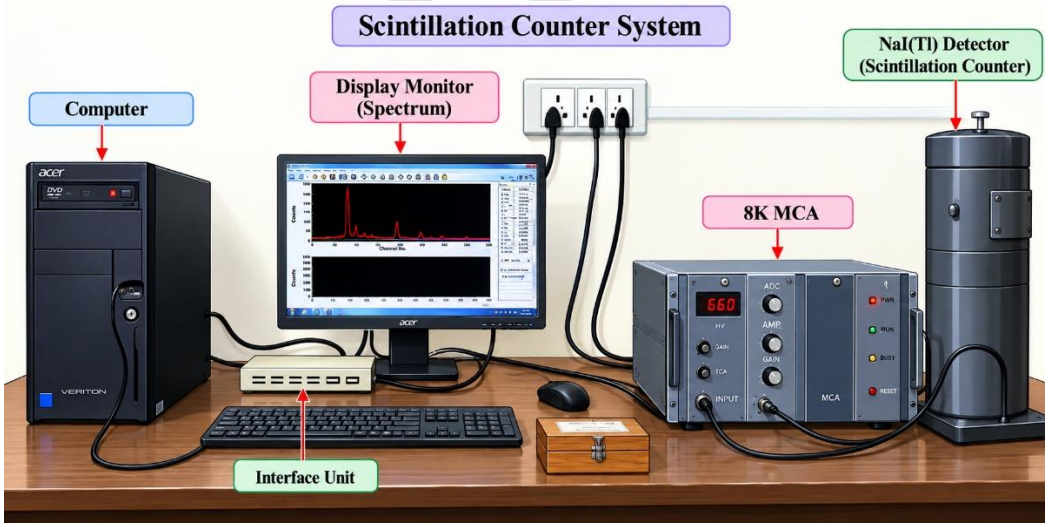


Fig. 1. Schematic diagram of NaI (Tl) Scintillation Detector setup.

3. Results and Discussion

3.1 Linear Attenuation Coefficient

Figure 2 shows the variation of the linear attenuation coefficient (LAC) of the investigated samples (S1–S4) as a function of photon energy in the range of 122–1330 keV. The LAC values were theoretically calculated using the Phy-X/PSD [23–25].

It is observed that the LAC values of all samples decrease with increasing photon energy. This trend is attributed to the dominant contribution of the photoelectric absorption process at low photon energies, where the probability of photon interaction is relatively high. As the photon energy increases, the contribution of Compton scattering becomes dominant, resulting in a gradual decrease in the attenuation coefficient [26].

Among the investigated samples, S4 exhibits the highest LAC values throughout the studied energy range, indicating superior gamma-ray attenuation capability. At 122 keV, the LAC values are 0.215, 0.229, 0.214, and 0.307 cm^{-1} for S1, S2, S3, and S4, respectively. The significantly higher attenuation observed for S4 is attributed to the presence of platinum (Pt), which possesses a high atomic number and consequently a higher probability for photoelectric interaction with incident photons [26].

At 356 keV, the LAC values decrease to 0.149, 0.159, 0.149, and 0.193 cm^{-1} for S1, S2, S3, and S4, respectively. A similar decreasing trend is observed at 511 keV, where the corresponding values are 0.129, 0.138, 0.128, and 0.142 cm^{-1}. Between 662 and 1173 keV, the attenuation coefficients continue to decrease gradually, reaching values of 0.115–0.145 cm^{-1} at 662 keV and 0.088–0.126 cm^{-1} at 1173 keV. This gradual reduction is mainly due to the predominance of Compton scattering, which depends less strongly on the atomic number of the shielding material than the photoelectric effect [27].

At the highest investigated energy of 1330 keV, the LAC values become very close, measuring 0.083, 0.089, 0.083, and 0.088 cm^{-1} for S1, S2, S3, and S4, respectively. The convergence of these values indicates that the influence of chemical composition on photon attenuation becomes less significant at higher energies, where Compton scattering is the primary interaction mechanism.

Overall, the shielding performance follows the order: S4 > S2 > S1 ≈ S3

throughout most of the investigated energy range. The consistently higher LAC values of S4 demonstrate that the incorporation of the platinum-containing compound significantly enhances gamma-ray attenuation compared with the other investigated biopolymeric materials. Therefore, S4 exhibits the best shielding performance among the studied samples and is the most suitable candidate for gamma-ray shielding applications.

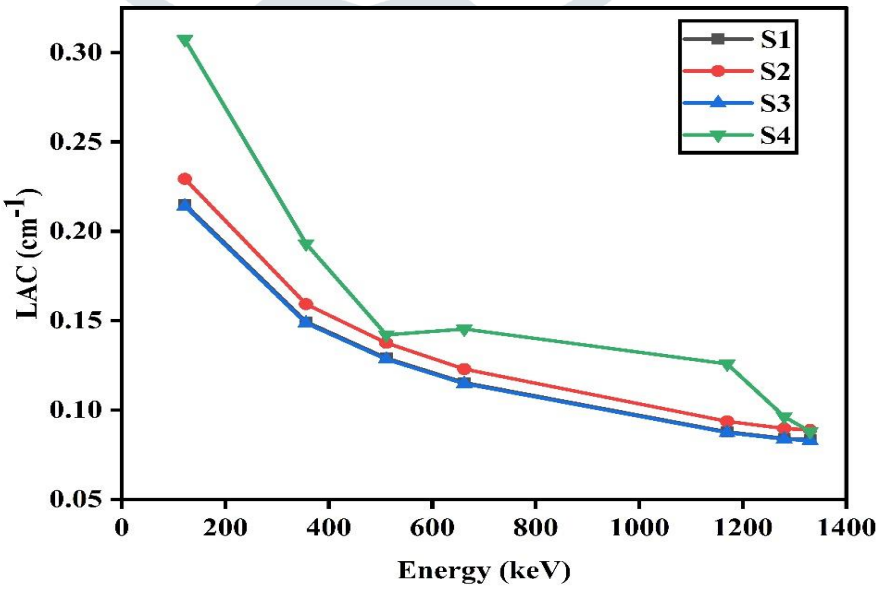


Fig. 2. The Linear Attenuation Coefficient (LAC) of Biopolymers.

3.2 Mass Attenuation Coefficient

The mass attenuation coefficient (MAC) of chitosan ($C_{56}H_{103}N_9O_{39}$), cellulose ($(C_6H_{10}O_5)_n$), starch ($(C_6H_{10}O_5)_n$), and cisplatin ($C_{12}H_6N_2Pt$) was evaluated over the photon energy range of 122–1330 keV using both theoretical calculations performed with the Phy-X/PSD software and experimental measurements. The theoretical and experimental MAC values for all investigated samples are presented in Table 1. In both approaches, the MAC values decrease continuously with increasing photon energy, which is consistent with the fundamental photon interaction mechanisms. At lower photon energies, photoelectric absorption predominates, resulting in higher attenuation coefficients, whereas Compton scattering becomes the dominant interaction process at intermediate energies. Above 1.022 MeV, pair production begins to contribute; however, its effect remains relatively small within the investigated energy range [28–32].

Table 1 The Mass Attenuation Coefficient (MAC) of Biopolymers.

Energy	S1 Phy-X	Exp	S2 Phy-X	Exp	S3 Phy-X	Exp	S4 Phy-X	Exp
122	0.116	0.091	0.145	0.115	0.153	0.136	1.686	1.496
356	0.097	0.074	0.106	0.088	0.126	0.102	0.185	0.158
511	0.092	0.068	0.097	0.071	0.105	0.078	0.118	0.101
662	0.082	0.052	0.094	0.063	0.093	0.065	0.108	0.082
1170	0.030	0.021	0.042	0.025	0.048	0.032	0.060	0.039
1280	0.028	0.018	0.041	0.02	0.047	0.028	0.057	0.033
1330	0.027	0.011	0.038	0.013	0.041	0.022	0.055	0.024

Among all the investigated materials, cisplatin (S4) exhibited the highest theoretical and experimental MAC values throughout the studied energy range. At 122 keV, the theoretical and experimental MAC values of cisplatin were 1.686 and 1.496 $cm^2\ g^{-1}$, respectively, which are considerably higher than those of the natural biopolymers. This superior attenuation capability is mainly attributed to the presence of platinum (Pt, Z = 78), whose high atomic number significantly enhances the photoelectric absorption probability at low photon energies [33]. For the natural biopolymers, starch (S3) showed the highest attenuation, followed by cellulose (S2) and chitosan (S1). At 122 keV, the experimental MAC values were 0.136, 0.115, and 0.091 $cm^2\ g^{-1}$ for starch, cellulose, and chitosan, respectively. The observed differences are associated with variations in elemental composition, density, and effective electron density of the investigated materials [34].

As the photon energy increased from 356 to 662 keV, both the theoretical and experimental MAC values gradually decreased for all samples. At 662 keV, the theoretical MAC values were 0.082, 0.094, 0.093, and 0.108 $cm^2\ g^{-1}$, while the corresponding experimental values were 0.052, 0.063, 0.065, and 0.082 $cm^2\ g^{-1}$ for chitosan, cellulose, starch, and cisplatin, respectively. This reduction is attributed to the predominance of Compton scattering, where photon attenuation becomes less dependent on the atomic number of the shielding material [32].

At higher photon energies (1170–1330 keV), both theoretical and experimental MAC values reached their minimum. At 1330 keV, the theoretical MAC values decreased to 0.027, 0.038, 0.041, and 0.055 $cm^2\ g^{-1}$, whereas the experimental values were 0.011, 0.013, 0.022, and 0.024 $cm^2\ g^{-1}$ for chitosan, cellulose, starch, and cisplatin, respectively. Although pair production becomes energetically possible above 1.022 MeV, its contribution is relatively limited for the investigated materials. Nevertheless, cisplatin maintained higher attenuation than the other samples because of the presence of high-Z platinum atoms [34].

A comparison of the theoretical and experimental results reveals that the theoretical MAC values obtained using Phy-X/PSD are consistently higher than the corresponding experimental values. These small discrepancies may be attributed to factors such as detector efficiency, counting statistics, sample thickness uncertainty, beam divergence, density variation, and experimental alignment errors [35]. Despite these minor deviations, both theoretical and experimental results exhibit the same energy-dependent trend and show good agreement throughout the investigated energy range, confirming the reliability of both the computational method and the experimental measurements.

Overall, the gamma-ray attenuation performance of the investigated materials follows the order: Cisplatin (S4) > Starch (S3) > Cellulose (S2) > Chitosan (S1).

The excellent agreement between the theoretical calculations and experimental measurements demonstrates the accuracy of the Phy-X/PSD software in predicting photon attenuation characteristics. Furthermore, the superior shielding performance of cisplatin confirms that incorporating high atomic number elements into biopolymeric materials significantly enhances gamma-ray attenuation, particularly in the low-energy region where photoelectric absorption dominates. These findings suggest that platinum-containing biopolymer composites have considerable potential for the development of efficient and environmentally friendly radiation shielding materials for medical, industrial, and nuclear
applications [36–38].

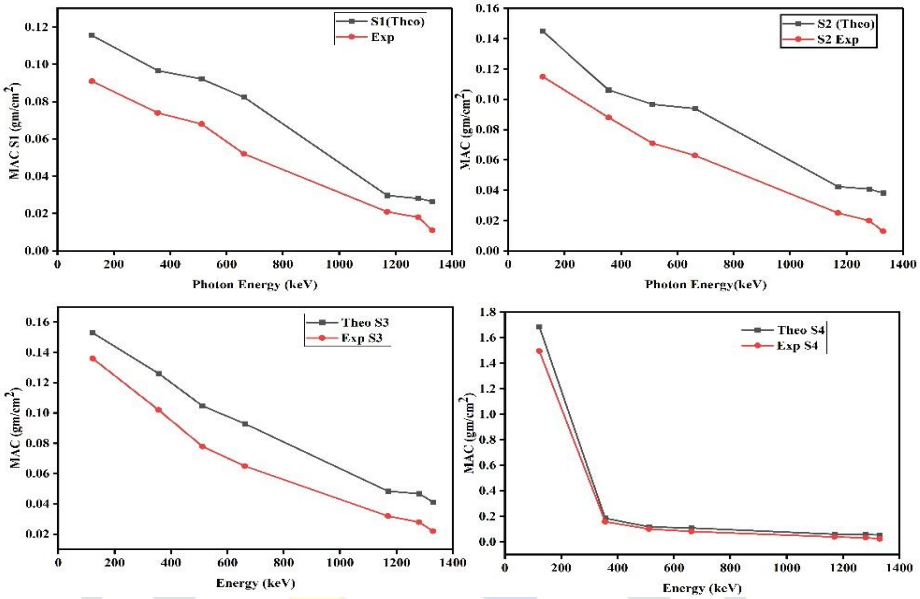


Fig. 3. Thermotical and Experimental Mass Attenuation Coefficient (MAC) of Biopolymers

3.3 Half Value Layer (HVL)

Figure 4 presents the variation of the half-value layer (HVL) of the investigated samples (S1–S4) as a function of photon energy in the range of 122–1330 keV. The HVL values were theoretically calculated using the Phy-X/PSD software based on the NIST XCOM photon cross-section database [39–40]. The half-value layer represents the thickness of a shielding material required to reduce the incident gamma-ray intensity to 50% of its original value. Therefore, materials with lower HVL values exhibit superior radiation shielding performance [41-42].

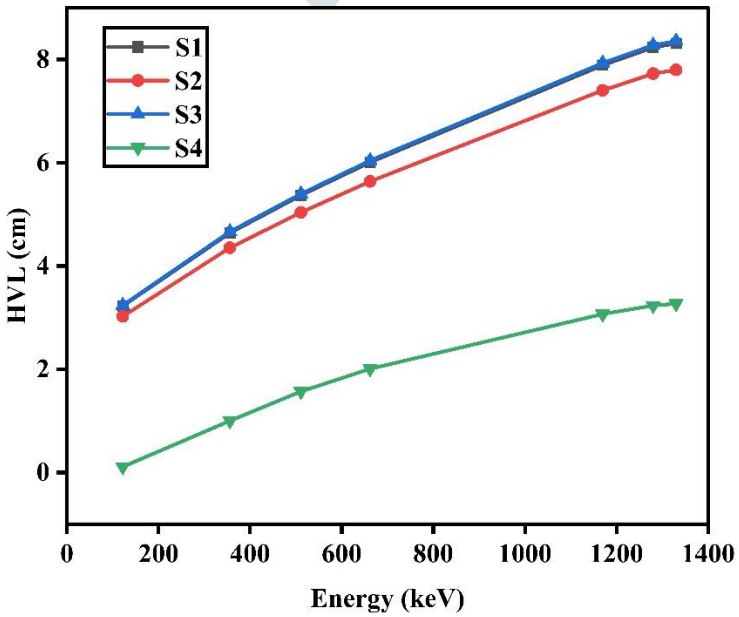


Fig. 4 Half Value Layer (HVL) of Biopolymers.

As shown in Figure 4, the HVL values increase steadily with increasing photon energy for all investigated samples. This increase is due to the decrease in photon interaction probability at higher energies, which requires a greater material thickness to achieve the same level of attenuation [43]. At 122 keV, the HVL values are 3.224, 3.023, 3.239, and 0.110 cm for S1, S2, S3, and S4, respectively. Sample S4 exhibits the lowest HVL value, indicating the highest shielding efficiency among all samples. As the energy increases to 356, 511, and 662 keV, the HVL values gradually increase, reaching 4.639–1.000 cm, 5.399–1.568 cm, and 6.042–2.007 cm for S1–S4, respectively.

At higher photon energies (1173–1330 keV), the HVL values continue to increase because Compton scattering becomes the dominant photon interaction mechanism. At 1330 keV, the HVL values reach 8.314, 7.801, 8.358, and 3.271 cm for S1, S2, S3, and S4, respectively. Although all samples exhibit increasing HVL with energy, S4 consistently maintains the lowest values throughout the investigated energy range, indicating that a comparatively smaller thickness is required for effective gamma-ray attenuation. The shielding performance based on HVL follows the order: S4 > S2 > S1 > S3.

The lower HVL values of S4 are attributed to the presence of platinum, which enhances photon attenuation due to its high atomic number. Consequently, S4 demonstrates the best shielding performance and can be considered the most suitable material among the investigated biopolymer-based samples for gamma-ray shielding applications.

3.4 TVL

Figure 5 shows the variation of the tenth-value layer (TVL) of the investigated samples (S1–S4) as a function of photon energy in the range of 122–1330 keV. The TVL values were calculated using the Phy-X/PSD software based on the NIST XCOM database [44–46]. The tenth-value layer represents the thickness of a material required to reduce the intensity of incident gamma radiation to one-tenth (10%) of its original value. Hence, lower TVL values indicate superior radiation shielding performance [47].

As illustrated in Figure 5, the TVL values increase with increasing photon energy for all the investigated samples. This behavior is attributed to the decrease in photon interaction probability at higher energies, resulting in a greater thickness of shielding material being required to attenuate the incident radiation [48]. At 122 keV, the TVL values are 10.711, 10.042, 10.759, and 0.365 cm for S1, S2, S3, and S4, respectively. Among all samples, S4 exhibits the lowest TVL value, indicating the highest shielding effectiveness.

With increasing photon energy, the TVL values increase gradually. At 356, 511, and 662 keV, the TVL values are 15.411–3.322 cm, 17.840–5.209 cm, and 19.964 – 6.667 cm for S1–S4, respectively. At higher photon energies of 1173, 1280, and 1330 keV, the TVL values further increase to 26.210–10.197 cm, 27.354–10.744 cm, and 27.618–10.865 cm, respectively. The continuous increase in TVL with energy is mainly associated with the dominance of Compton scattering, which reduces the attenuation capability of the materials at higher photon energies.

Among the investigated samples, S4 consistently exhibits the lowest TVL values throughout the studied energy range, whereas S3 shows the highest values. The shielding performance based on the TVL values follows the order: S4 > S2 > S1 > S3.

The significantly lower TVL values of S4 indicate that a much smaller thickness is required to achieve 90% attenuation of gamma radiation compared to the other samples. This superior shielding performance is attributed to the presence of platinum in S4, which enhances photon attenuation owing to its high atomic number. Therefore, S4 can be considered the most effective shielding material among the investigated biopolymer-based samples.

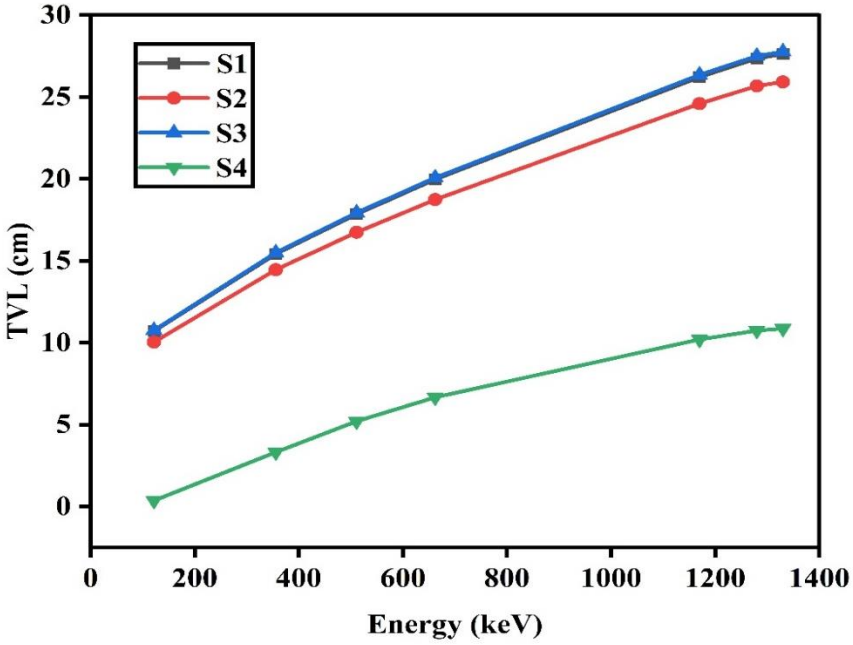


Figure 5. Variation of the Tenth-Value Layer (TVL) of Biopolymers (S1–S4) as a function of photon energy (122–1330 keV), calculated using the Phy-X/PSD software.

3.5 Mean Free Path (MFP)

Figure 6 shows the variation of the mean free path (MFP) of the investigated samples (S1–S4) as a function of photon energy in the range of 122–1330 keV. The MFP values were calculated using the Phy-X/PSD software based on the NIST XCOM photon cross-section database [49–51]. The mean free path represents the average distance travelled by a gamma photon before undergoing an interaction with the shielding material. Therefore, lower MFP values indicate a higher probability of photon interaction and consequently better shielding performance [52].

As illustrated in Figure 4, the MFP values increase progressively with increasing photon energy for all investigated samples. This trend is attributed to the reduction in photon interaction probability at higher energies, allowing gamma photons to penetrate further into the material before interacting [53]. At 122 keV, the MFP values are 4.652, 4.361, 4.673, and 0.159 cm for S1, S2, S3, and S4, respectively. Sample S4 exhibits the lowest MFP value, indicating superior attenuation capability compared to the other investigated samples.

With increasing photon energy, the MFP values gradually increase. At 356, 511, and 662 keV, the MFP values are 6.693–1.443 cm, 7.748–2.262 cm, and 8.670–2.896 cm for S1–S4, respectively. At higher photon energies of 1173, 1280, and 1330 keV, the MFP values further increase to 11.383–4.428 cm, 11.880–4.666 cm, and 11.994–4.719 cm, respectively. The increase in MFP at higher energies reflects the dominance of Compton scattering, which decreases the interaction probability of photons with the shielding materials[54-56].

Among the investigated samples, S4 consistently exhibits the lowest MFP values over the entire energy range, while S3 shows the highest values. The shielding performance based on MFP follows the order: S4 > S2 > S1 > S3.

The lower MFP values of S4 indicate that gamma photons travel a shorter distance before interaction, confirming its superior radiation attenuation capability. This improved shielding performance is mainly attributed to the presence of platinum in the material, whose high atomic number enhances photon absorption. Consequently, S4 is the most effective shielding material among the investigated biopolymer-based samples for gamma-ray protection.

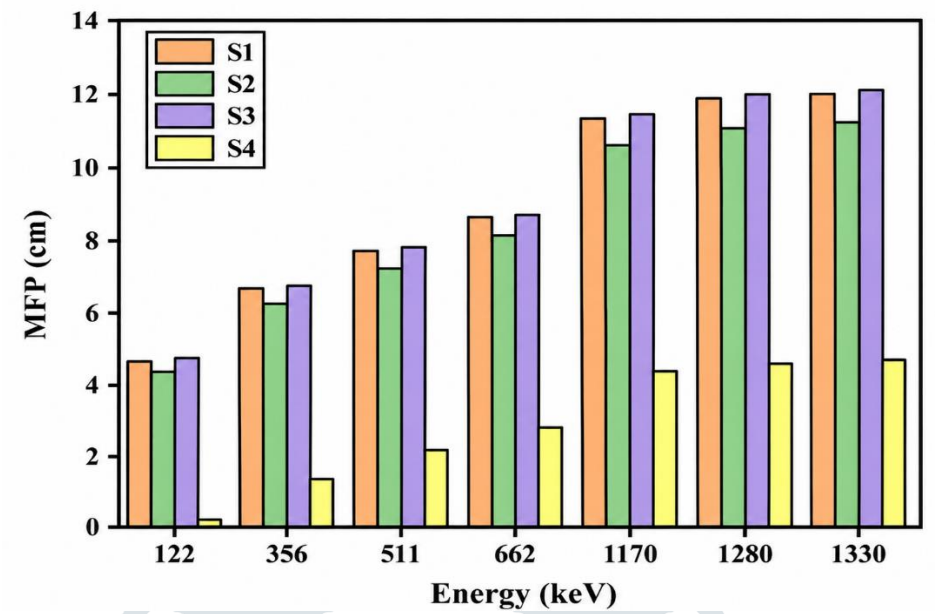


Figure 6. The Mean Free Path (MFP) of Biopolymers.

4. Conclusion

In the present study, the gamma-ray shielding performance of chitosan (S1), cellulose (S2), starch (S3), and cisplatin (S4) was theoretically investigated using the Phy-X/PSD software in the photon energy range of 122–1330 keV. The radiation shielding parameters, including the mass attenuation coefficient (MAC), linear attenuation coefficient (LAC), half-value layer (HVL), tenth-value layer (TVL), and mean free path (MFP), were evaluated to assess the shielding efficiency of the selected biopolymeric materials.

The obtained results revealed that the attenuation coefficients (MAC and LAC) decreased with increasing photon energy, whereas the shielding thickness parameters (HVL, TVL, and MFP) increased over the investigated energy range due to the transition from photoelectric absorption to Compton scattering as the dominant photon interaction mechanism. Among the investigated samples, S4 consistently exhibited the highest MAC and LAC values together with the lowest HVL, TVL, and MFP values, demonstrating superior gamma-ray attenuation capability. In contrast, S1, S2, and S3 showed comparatively lower shielding performance, with S2 performing slightly better than S1 and S3 at most photon energies.

The enhanced shielding performance of S4 is mainly attributed to the presence of platinum (Pt), a high atomic number element that significantly increases the probability of photon interaction, particularly at lower photon energies. The results indicate that incorporating heavy-metal-containing compounds into biopolymer matrices can substantially improve radiation attenuation while maintaining the advantages of polymer-based materials.

Overall, the present investigation demonstrates that cisplatin-based biopolymeric material (S4) possesses excellent gamma-ray shielding characteristics and can be considered a promising candidate for lightweight and environmentally friendly radiation shielding applications in medical, industrial, and nuclear technologies. Furthermore, the theoretical results obtained using the Phy-X/PSD software provide a useful basis for future experimental investigations and the development of advanced biopolymer-based radiation shielding materials.

Acknowledgments: One of the authors, Miss. Kanchan R. Niras would like to thank Chhatrapati Shahu Maharaj Research Training and Human Development Institute (SARTHI), Pune (Govt. of Maharashtra, India) for the financial support under the scheme CSMNRF. (Ref.no. SARTHI/Scholarship/CSMNRF-2022/2022-23/2341).

5. References

1.Sayyed, M.I., Tekin, H.O., Agar, O., Kılıçarslan, S., Alım, B., Radiation shielding properties of polymer composites, Radiation Physics and Chemistry 150 (2018) 257–264.

2.Akkurt, I., Akyıldırım, H., Mavi, B., Kılıçarslan, S., Başyiğit, C., Gamma-ray shielding properties of concrete including barite at different energies, Progress in Nuclear Energy 52 (2010) 620–623.

3.Akkurt, I., Başyiğit, C., Kılıçarslan, S., Mavi, B., Akkurt, A., Radiation shielding of concretes containing different aggregates, Cement and Concrete Composites 28 (2006) 153–157.
4.Akkurt, I., Başyiğit, C., Kılıçarslan, S., Mavi, B., The shielding of γ-rays by concretes produced with barite, Progress in Nuclear Energy 46 (2005) 1–11.
5.El-Khayatt, A.M., Radiation shielding characteristics of heavyweight concrete, Annals of Nuclear Energy 37 (2010) 991–995.
6.Bashter, I.I., Calculation of radiation attenuation coefficients for shielding concretes, Annals of Nuclear Energy 24 (1997) 1389–1401.
7.Elmahroug, Y., Tellili, B., Souga, C., Determination of gamma-ray shielding parameters for different materials using Monte Carlo simulation and XCOM data, Applied Radiation and Isotopes 70 (2012) 355–358.
8.Singh, V.P., Badiger, N.M., Kaewkhao, J., Radiation shielding properties of bismuth borate glasses, Radiation Physics and Chemistry 81 (2012) 1050–1053.
9.Chanthima, N., Kaewkhao, J., Investigation on radiation shielding parameters of bismuth borosilicate glass from 1 keV to 100 GeV, Annals of Nuclear Energy 55 (2013) 23–28.
10. Singh, H., Singh, T., Sharma, A., Singh, P.S., Mudahar, G.S., Gamma-ray attenuation coefficients in bismuth borate glasses, Annals of Nuclear Energy 35 (2008) 1191–1194.
11. Kaewkhao, J., Limsuwan, P., Mass attenuation coefficients and effective atomic numbers of phosphate glasses containing heavy metal oxides, Progress in Nuclear Energy 52 (2010) 580–584.
12. Manohara, S.R., Hanagodimath, S.M., Gerward, L., Photon interaction studies in materials of dosimetric interest, Applied Radiation and Isotopes 66 (2008) 1684–1693.
13. Kaewkhao, J., Chanthima, N., Limsuwan, P., Gamma-ray shielding properties of lead-bismuth borate glasses, Annals of Nuclear Energy 38 (2011) 1438–1441.
14. Akkurt, I., Akyıldırım, H., Mavi, B., Kılıçarslan, S., Başyiğit, C., Radiation shielding of concrete containing zeolite, Radiation Measurements 46 (2011) 827–830.
15. Akkurt, I., Akyıldırım, H., Mavi, B., Kılıçarslan, S., Başyiğit, C., Gamma-ray shielding properties of concrete including barite at different energies, Progress in Nuclear Energy 52 (2010) 620–623.
16. Akkurt, I., Akyıldırım, H., Mavi, B., Kılıçarslan, S., Başyiğit, C., Gamma-ray shielding properties of concrete containing different aggregates, Annals of Nuclear Energy 37 (2010) 910–914.
17. Demir, F., Budak, G., Şahin, R., Karabulut, A., Oltulu, M., Ün, A., Determination of radiation attenuation coefficients of heavyweight- and normal-weight concretes containing colemanite and barite for 0.663 MeV γ-rays, Annals of Nuclear Energy 38 (2011) 1274–1278.
18. Akkurt, I., Başyiğit, C., Kılıçarslan, S., Mavi, B., Akkurt, A., Radiation shielding of concretes containing different aggregates, Cement and Concrete Composites 28 (2006) 153–157.
19. Basyigit, C., Kılıçarslan, S., Akkurt, I., Mavi, B., Altindag, R., Akkurt, A., Karaguzel, R., The effect of freezing-thawing cycles on the radiation shielding properties of concretes, Building and Environment 41 (2006) 1070–1073.
20. Akkurt, I., Mavi, B., Akkurt, A., Başyiğit, C., Kılıçarslan, S., Yalım, H.A., Study on Z dependence of partial and total mass attenuation coefficients, Journal of Quantitative Spectroscopy and Radiative Transfer (2005) 379–385.
21. Akkurt, I., Kılıçarslan, S., Başyiğit, C., The photon attenuation coefficients of barite, marble and limra, Annals of Nuclear Energy 31 (2004) 577–582.
22. Oto, B., Yıldız, N., Akdemir, F., Kavaz, E., Investigation of gamma radiation shielding properties of various ores, Progress in Nuclear Energy 85 (2015) 391–403.
23. Waly, E.S.A., Bourham, M.A., Comparative study of different concrete composition as gamma-ray shielding materials, Annals of Nuclear Energy 85 (2015) 306–310.
24. Akkurt, I., El-Khayatt, A.M., The effect of barite proportion on neutron and gamma-ray shielding, Annals of Nuclear Energy 51 (2013) 5–9.

25. Akkurt, I., Akyıldırım, H., Radiation transmission of concrete including pumice for 662, 1173 and 1332 keV gamma rays, Nuclear Engineering and Design 252 (2012) 163–166.
26. El-Khayatt, A.M., Akkurt, I., Photon interaction, energy absorption and neutron removal cross section of concrete including marble, Annals of Nuclear Energy 60 (2013) 8–14.
27. Akman, F., Khattari, Z.Y., Kaçal, M.R., Sayyed, M.I., Afaneh, F., The radiation shielding features for some silicide, boride and oxide type ceramics, Radiation Physics and Chemistry 160 (2019) 9–14.
28. Yasaka, P., Pattanaboonmee, N., Kim, H.J., Limkitjaroenporn, P., Kaewkhao, J., Gamma radiation shielding and optical properties measurements of zinc bismuth borate glasses, Annals of Nuclear Energy 68 (2014) 4–9.
29. Lokhande, R.M., Vinayak, V., Mukhamale, S.V., Khirade, P.P., Gamma radiation shielding characteristics of various spinel ferrite nanocrystals: a combined experimental and theoretical investigation, RSC Advances 11 (2021) 7925–7937.
30. Gaikwad, K.B., Gattu, K.P., More, C.V., Pawar, P.P., Physical, structural and nuclear radiation shielding behavior of Ni–Cu–Zn Fe_2O_4 ferrite nanoparticles, Applied Radiation and Isotopes 207 (2024) 111244.
31. Gaikwad, K.B., Gattu, K.P., More, C.V., Sayyed, M.I., Niras, K.R., Pawar, P.P., Experimental evaluation of gamma radiation attenuation properties of $Ni_{0.2}Mg_xZn_{0.8-x}Fe_2O_4$ ferrites, Optical Materials 148 (2024) 114807.
32. Gaikwad, K.B., Radiation shielding properties of some transition metal salts, Journal of Emerging Technologies and Innovative Research 12 (2025) f628–f635.
33. Gaikwad, K.B., Gattu, K.P., Obaid, S.S., Pawar, P.P., Comparative study of radiation shielding parameters for $NiFe_2O_4$ and $CoFe_2O_4$ nanoparticles, AIP Conference Proceedings 3149 (2024) 020014.
34. Reddy, B.C., Manjunatha, H.C., Vidya, Y.S., Manjunatha, S., Sridhar, K.N., Seenappa, L., Munirathnam, R., Thirunavukkarasu, V., Spinel manganese nanoferrite for X-ray/gamma radiation shielding, display and antimicrobial applications, Physica B: Condensed Matter 661 (2023) 414835.
35. Al-Buriahi, M.S., Olarinoye, I.O., Yılmaz, E., Çalışkan, F., Sriwunkum, C., Evaluation of the structural and radiation transmission parameters of recycled borosilicate waste glass system: An effective material for nuclear shielding, Annals of Nuclear Energy 213 (2025) 111136.
36. Sangwaranatee, N.W., Cheewasukhanont, W., Limkitjaroenporn, P., Borisut, P., Wongdamnern, N., Khrongchaiyaphum, F., Kothan, S., Kaewkhao, J., Development of bismuth alumino borosilicate glass for radiation shielding material, Radiation Physics and Chemistry 186 (2021) 109542.
37. Akkurt, I., Malidarre, R.B., Kavas, T., Monte Carlo simulation of radiation shielding properties of the glass system containing Bi_2O_3, European Physical Journal Plus 136 (2021) 264.
38. Akkurt, I., Günüoğlu, K., Kurtuluş, R., Kavas, T., X-ray shielding parameters of lanthanum oxide added waste soda-lime glass, X-Ray Spectrometry 50 (2021) 168–179.
39. Ali, M.A.E.M., Tawfic, A.F., Abdelgawad, M.A., Wagih, M., Omar, A., Potential uses of different sustainable concrete mixtures in gamma and neutrons shielding purposes, Progress in Nuclear Energy 157 (2023) 104598.
40. Akkurt, I., Başyiğit, C., Kılıçarslan, S., Mavi, B., The shielding of γ-rays by concrete produced with barite, Progress in Nuclear Energy 46 (2005) 1–11.
41. Aksoğan, O., Binici, H., Örtlek, E., Durability of concrete made by partial replacement of fine aggregate by colemanite and barite and cement by ashes of corn stalk, wheat straw and sunflower stalk ashes, Construction and Building Materials 106 (2016) 253–263.
42. Al-Hadeethi, Y., et al., A comprehensive study on the effect of TeO_2 on the radiation shielding properties of TeO_2–B_2O_3–Bi_2O_3–LiF–$SrCl_2$ glass system using Phy-X/PS software, Ceramics International.
43. Al-Buriahi, M.S., et al., Physical properties and gamma radiation shielding capability of highly dense binary bismuth borate glasses, Ceramics International 47 (2021) 9791–9805.
44. Oto, B., Gür, A., Gür, M., Aygün, B., Sayyed, M.I., Gamma-ray shielding properties of various ores, Progress in Nuclear Energy 85 (2015) 391–403.

45. Stanković, S.J., Ilić, R.D., Janković, K., Bojović, D., Lončar, B., Gamma-ray shielding properties of concrete, Radiation Measurements.
46. Demir, F., Budak, G., Şahin, R., Karabulut, A., Oltulu, M., Ün, A., Determination of radiation attenuation coefficients of heavyweight- and normal-weight concretes containing colemanite and barite for 0.663 MeV γ-rays, Annals of Nuclear Energy 38 (2011) 1274–1278.
47. Akman, F., Kaçal, M.R., Sayyed, M.I., Tekin, H.O., Investigation of gamma-ray shielding parameters of some materials, Radiation Physics and Chemistry.
48. Kaewkhao, J., Limsuwan, P., Mass attenuation coefficients and effective atomic numbers in phosphate glass containing Bi_2O_3, PbO and BaO at 662 keV, Nuclear Instruments and Methods in Physics Research Section A 619 (2010) 295–297.
49. Saeed, A., El Shazly, R., Elbashar, Y.H., Abou El-Azm, A.M., Gamma ray attenuation in a developed borate glassy system, Radiation Physics and Chemistry 102 (2014) 167–170.
50. Ouis, M.A., ElBatal, F.H., Shielding behavior of MoO_3-doped lead borate glasses towards gamma irradiation assessed through collective optical, FTIR, and ESR spectral analysis, Radiation Physics and Chemistry 191 (2022) 109537.
51. Teresa, P.E., Naseer, K.A., Marimuthu, K., Alavian, H., Sayyed, M.I., Influence of modifiers on the physical, structural, elastic and radiation shielding competence of Dy^{3+} ions doped alkali boro-tellurite glasses, Radiation Physics and Chemistry 190 (2022) 109741.
52. E. Kavaz, An experimental study on gamma-ray shielding features of lithium borate glasses doped with dolomite, hematite and goethite minerals, Radiation Physics and Chemistry 160 (2019) 112–123.
53. O.I. Sallam, A.M. Madbouly, N.A. Elalaily, F.M. Ezz-Eldin, Physical properties and radiation shielding parameters of bismuth borate glasses doped transition metals, Journal of Alloys and Compounds 843 (2020) 156056.
54. Gaikwad, K.B., More, C.V., Gattu, K.P., Niras, K.R., Obaid, S.S., Pawar, P.P., Comparative study of radiation shielding parameters for $CoZnFe_2O_4$ and $CuZnFe_2O_4$ nanoparticles, Radiation Effects and Defects in Solids (2025), 1–15.
55. Gaikwad, K.B., Algethami, M., More, C.V., Sayyed, M.I., Pawar, P.P., Enhanced radiation shielding properties of advanced ceramic materials, Journal of Alloys and Compounds 1033 (2025) 181384.
56. Gaikwad, K.B., Gattu, K.P., More, C.V., Ogul, H., Pawar, P.P., Gamma-ray shielding features of $Co_{1-x}Cu_xFe_2O_4$ ferrite: A combined experimental, theoretical and simulation investigation, Radiation Physics and Chemistry 224 (2024) 111996.